Journal of Applied Polymer Science

Dye Removal from Colored-Textile Wastewater using Chitosan-PPI Dendrimer Hybrid as a Biopolymer: Optimization, Kinetic, and Isotherm Studies

Mousa Sadeghi-Kiakhani,[1] Mokhtar Arami,[1] Kamaladin Gharanjig[2]
[1]Department of Textile Engineering, Amirkabir University of Technology, Tehran, Iran
[2]Department of Organic Colorants, Institute for Color Science and Technology, Tehran, Iran
Correspondence to: M. Arami (E-mail: arami@aut.ac.ir)

ABSTRACT: Preparation of a biopolymer chitosan-polypropylene imine (CS-PPI) as a biocompatible adsorbent and its reactive textile dyes removal potential were performed. Chemical specifications of CS-PPI were determined using Fourier transform infrared, ^{1}H-NMR, and ^{13}C-NMR. The surface morphology of the CS-PPI surface was characterized by scanning electron microscopy. Results confirmed that the linkages between the NH_2 groups of PPI dendrimer and carboxylic groups of modified Chitosan were accomplished chemically. Two textile reactive dyes, reactive black 5 (RB5) and reactive red 198 (RR198), were used as model compounds. A response surface methodology was applied to estimate the simple and combined effects of the operating variables, including pH, dye concentration, time contact, and temperature. Under the optimal values of process parameters, the dye removal performance of 97 and 99% was achieved for RB5 and RR198, respectively. Furthermore, the isotherm and kinetic models of dyes adsorption were performed. Adsorption data represented that both examined dye followed the Langmuir isotherm. The adsorption kinetics of both reactive dyes were satisfied by pseudo-second order equation. Based on this study, CS-PPI due to having high adsorption capacity (6250 mg/g for RB5 and 5882.35 mg/g for RR198), biocompatibility and ecofriendly properties might be a suitable adsorbent for removal of reactive dyes from colored solutions. © 2012 Wiley Periodicals, Inc. J. Appl. Polym. Sci. 000: 000–000, 2012

KEYWORDS: biopolymer; chitosan–dendrimer; reactive dyes; isotherm adsorption; kinetics models

Received 29 October 2011; accepted 31 January 2012; published online
DOI: 10.1002/app.37615

INTRODUCTION

The presence of colored compounds to natural water resources is not only aesthetically undesirable but also it has a more serious environmental impact. Over a hundred thousand commercially available dyes to exist and more than 7×10^5 tons are produced annually.[1] Consequently, large quantities of dyes are introduced to the effluents from various industries, such as the textiles, leather, paper, plastics, food industries, etc.[2] The textile dyeing units consume large quantities of water at different steps of dyeing and finishing among other processes. Since a very small amount of dye in water is highly visible and can be toxic to creatures in water, the removal of dye from wastewater becomes environmentally essential.[3–12] The reactive textile dye effluent has more pollution than other textile dyes effluents due to their hydrolysis property in water. Almost 10–50% of all used reactive dyes after dyeing of textile goods such as cotton, wool, and polyamide remain in effluent.[13] For this reason, the elimination of reactive dyes from effluent is very essential for prevention of entrance of colored hazardous materials to nature.

Various methods have been developed to remove color from effluent, varying in performance, cost-effective, and ecological aspects. Adsorption is found to be a good technique to treat the polluted industrial waste effluents. It has considerable advantages in comparison to conventional methods, particularly from the technical, economic, and environmental point of views.[14–17] Many adsorbents have been experienced on the possibility to eliminate dye from textile effluents.[18] For obtaining high-performance adsorbent, it is crucial to select the more efficient and cheaper adsorbents by higher adsorption ability. Lately, chitosan has been reported to have the high potential of the adsorption capacity towards textile dyes in aqueous wastes.[19–21]

Chitosan is a natural cationic polysaccharide easily produced from the shells of crabs, shrimps, and prawns. Due to being nontoxic, antibacterial, and biodegradable, the chitosan and its derivatives have attracted more and more attention.[18] Chitosan

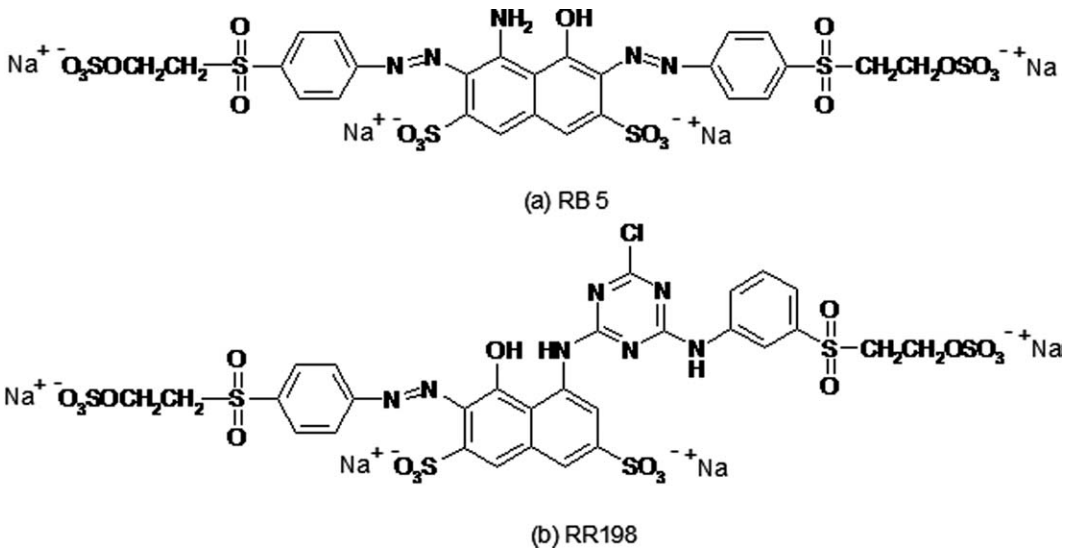

Figure 1. The chemical structure of the studied reactive dyes: (a): RB5; (b): RR198.

has a very high affinity for the majority of dye groups such as reactive, direct, and disperse, showing a lack of affinity only for basic dyes.[19–24] Furthermore, various chitosan composites containing nanoparticle such as chitosan/TiO_2, chitosan/cuprous oxide, chitosan/CdS, and chitosan/ZnO were prepared and used to remove different organic compounds.[12,25–27] Also, dendrimers are one of the significant groups of nanoarchitecture materials which can be used for extending of applications and more performance of chitosan.[28–34]

Dendrimers are a group of highly branched polymer compounds having different functional groups where they can react with different functional entities of other molecules in nanometer scale. Compared with polymers, dendrimers possess especial physical properties such as viscosity, flexibility, and density distribution.[15,16] For the particular envisaged properties; the distribution of functional groups in the dendrimer skeleton plays a significant role.[35–37] Generally, two diverse synthetic strategies are currently explored to synthesize structurally well-defined dendritic polymers, namely the divergent and convergent growth approaches.[38–41] Dendrimers are also attractive molecules due to their multifunctional properties and are potentially useful for textile applications.[38,39,42,43]

RSM is a practical statistical method in the adsorption for optimizing the process when a combination of several independent variables and their interactions affect desired responses.[44] By RSM, several variables are tested simultaneously with a minimum number of trials according to individual experimental designs based on factorial designs. The application of statistical experimental design methods in adsorption process development can result in improved process yields, reduced process variability, closer confirmation of the output response to nominal and target requirements, and reduced development time and overall costs.[45]

Literature review demonstrated that the CS-PPI nanoarchitecture was not applied to remove of textile dyes from colored solutions. This article represents in details the preparation, characterization, and dye adsorption properties of biocompatible polymer (CS-PPI). Chemical characteristics of CS-PPI were analyzed. Two textile reactive dyes were used as pollutant compounds. In addition, the optimization of operational conditions for CS-PPI using RSM to develop a mathematical correlation between operating variables for RB5 and RR198 dyes removal was evaluated. Furthermore, the kinetic and isotherm models of dyes adsorption were studied.

MATERIALS AND METHODS

Materials

Chitosan (extracted from snow crab shell, degree of deacetylation: 98.5%; average molecular weight: 200 kDa) was supplied by Kitotak Co. Ethyl acrylate (Ea) was provided from Merck. All solvents and materials were of analytical grade. Dialysis membranes (M_W 12,000 cutoff) and poly propylene imine (PPI), Generation 2 ($G = 2$), were purchased from Sigma Co. Reactive black 5 (RR5) and reactive red 198 (RR198) with a molecular weight of 991.82 g/mol and 968.21 g/mol, respectively, which were supplied by CIBA Co. (Figure 1).

Methods of Characterization

FTIR spectra were recorded on a Perkin-Elmer instrument using KBr pellets containing the prepared materials. The spectra presented are baseline corrected and converted to absorbance mode. The ^{1}H-NMR and ^{13}C-NMR spectra were obtained on a Brucker DRE AVANCE-500 MHz. Scanning electron microscope (SEM) of raw CS-PPI and dye adsorbed CS-PPI were obtained using LEO 1455VP scanning microscope. Adsorbent samples were removed from the dye solution after equilibration and separated from the water by drying at 30°C for 48 h in preparation for the SEM analysis.

Synthesis of Chitosan-Ethyl Acrylate

Optimum reaction parameters were used for the grafting of Ea onto chitosan.[46] Chitosan **1** (5 g) was dissolved in aqueous solution, containing acetic acid 37% (1.5 mL) and water/methanol 40/40 (80 mL). Ethyl acrylate (10 equiv/NH_2 in chitosan, 0.5 mL) was added to the solution. After stirring at 50°C for 10 days, an

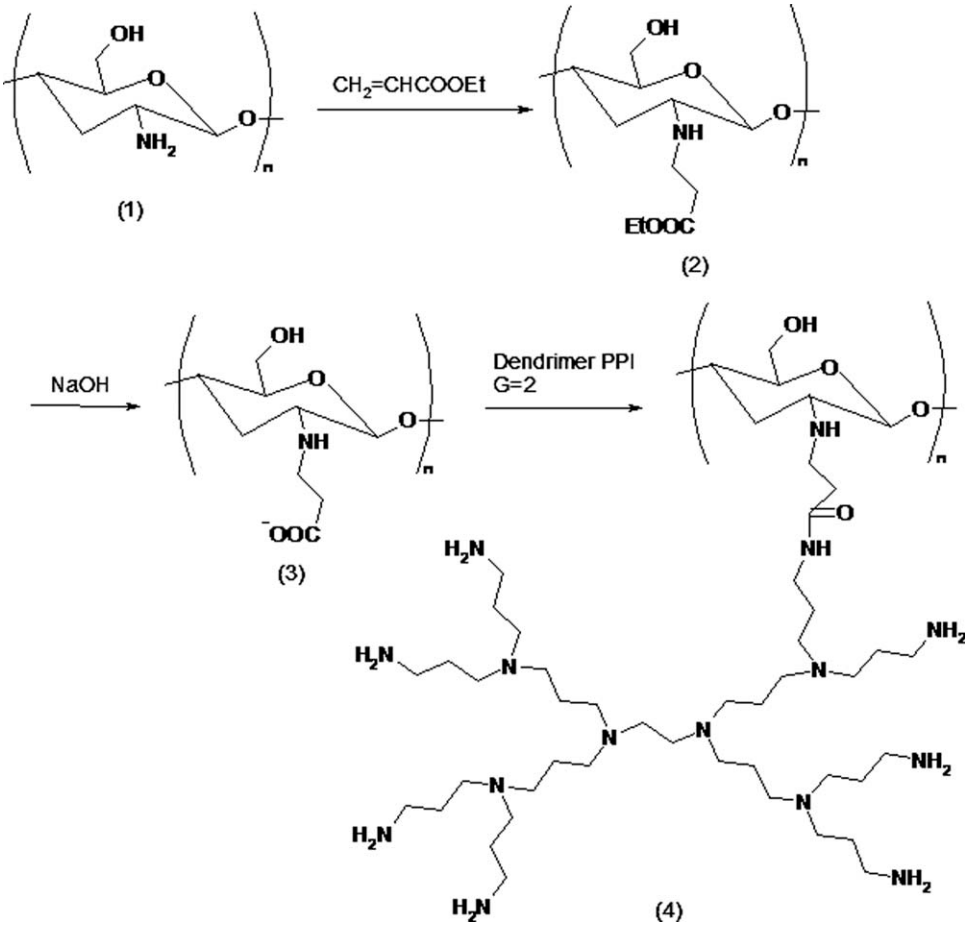

Figure 2. Scheme of the CS-PPI preparation.

aliquot of the reaction mixture was quenched by precipitation in acetone (80 mL) with saturated $NaHCO_3$. The precipitate was collected by filtration, dispersed in H_2O with saturated $NaHCO_3$ (20 mL), and the mixture was dialyzed against H_2O (4 L) for 2 days and lyophilized to give *N*-carboxyethyl chitosan ethyl ester (Ch-g-Ea) **2** (Figure 2). To obtain *N*-carboxyethyl chitosan **3**, 0.1% NaOH (50 mL) was added to **2**, the mixture was stirred for 2 h, dialyzed, and lyophilized as above. The precipitated powders were obtained in quantitative yield (95%).

Synthesis of Chitosan-PPI Hybrid

N-carboxyethylchitosan **3** (**3**: 100 mg) was dispersed in methanol (50 mL). PPI ($G = 2$) (0.54 mmol) was added to the prepared suspension. The mixture was stirred at room ambient. After 3 days, the mixture was evaporated to dryness, dispersed in 0.2 M NaOH at room temperature for 2 h, dialyzed, and lyophilized to give **4** (Figure 2).[33] All prepared products were ground to fine powders of between 0.2 and 0.4 mm.

Adsorption Study

The dye adsorption measurements were fulfilled by mixing a fixed amount of CS-PPI (0.001 g) for RB5 and RR198 in jars containing 50 mL of a dye solution (25–125 mg/L) at various pH_0 (2–10) and temperatures (30–50°C). pH solution was adjusted by H_2SO_4 or NaOH. At the end of the adsorption experiment, the solution samples were centrifuged at 4000 rpm for 10 min, and then the dye concentration was calculated. The maximum wavelength (λ_{max}) used for the determination of residual concentration of RB5 and RR198 in solution using UV–vis spectrophotometer were 599 and 520 nm, respectively. UV–vis spectrophotometer CECIL 2021 was utilized for absorbance measurements of solutions.

Experimental Design and Data Analysis

In this study, a central composite design (CCD) was used to determine the optimum condition for the dye removal by CS-PPI. The statistical software "MiniTab," version 16 was applied for CCD and the obtained data analyzing.

Experiments were carried out to determine a narrower range of pH, time duration, adsorbent dosage, and temperature prior to designing the experimental runs. For this reason, experiments were carried out by varying a single factor while keeping all other factors fixed at a specific set of condition. According to the obtained experimental data, levels of four main parameters investigated in this study are presented in Table I. Initial pH, concentration of dye, time contact, and temperature processes were chosen as four independent variables in the dye removal process. As a result, the CCD matrixes of 31 experiments covering full design of 5-level factors were used to build quadratic models as shown in Table I.

The value 2 of α was chosen to achieve rotatability. Rotatable designs provide the desirable property of constant forecast variance at all points that are equidistant from the design center, hence improving the quality of the forecast. The treatment of the

Table I. Experimental Range and Levels of Independent Process Variables

Independent variable	Factor x_i	Range and level				
		$-\alpha$	−1	0	1	$+\alpha$
Initial pH	X_1	−2	4	6	8	+2
C_{dye} (mg/L)	X_2	25	50	75	100	125
Time contact (min)	X_3	10	20	30	40	50
Temperature (°C)	X_4	30	35	40	45	50

dyes removal process is clarified by the following empirical second-order polynomial model Eq. (1):

$$\eta_i = b_0 + \sum_{i=1}^{n} b_i x_i + \sum_{i=1}^{n} b_{ii} x_i^2 + \sum_{i=1}^{n-1} \sum_{i=1}^{n} b_{ij} x_i x_j \qquad (1)$$

where η is the dye removal performance, b_0 the constant coefficient, b_i the linear coefficients, b_{ii} the quadratic coefficients, b_{ij} the interaction coefficients and x_i, x_j are the coded values of the variables. The statistical importance of the models was justified through the analysis of the variance (ANOVA) for polynomial models with 95% confidence level and residual plots were utilized to study the suitability of the models' fit. The quality of the fit polynomial model was expressed by the coefficient of determination R^2. The R^2 values provide a measure of how much variability in the observed response values can be explained by the experimental factors and their interactions. At last, the optimal values of the critical parameters were obtained by analyzing surface plots and also by searching a module in dedicated RSM program for a combination of factor levels that satisfy the requirements placed on the response. Experimental

Table II. Full Factorial Central Composite Design Matrix for RB5 and RR198 Removal (The Operational Variables Showed the Coded Value)

Observations	Initial pH	C_{dye} (mg/L)	Time contact (min)	Temperature (°C)	Dye removal efficiency (%)			
					RB5		RR198	
					Exp.	Pred.	Exp.	Pred.
1	0	0	0	2	52.57	48.99	73.27	64.07
2	0	0	0	0	47.91	47.81	68.44	68.40
3	1	−1	1	−1	16.55	19.96	22.58	28.29
4	0	0	0	0	47.81	47.81	68.44	68.40
5	1	1	1	−1	11.93	15.01	18.62	23.53
6	2	0	0	0	1.99	−11.36	2.38	−12.64
7	0	2	0	0	35.61	31.74	47.13	45.57
8	−2	0	0	0	96.98	103.86	99.38	103.69
9	0	0	0	−2	39.27	36.37	53.27	51.74
10	−1	−1	1	1	91.62	90.26	92.83	95.83
11	0	0	0	0	47.91	47.81	68.29	68.40
12	1	1	−1	1	8.37	14.47	15.62	18.71
13	−1	−1	−1	1	83.44	83.56	89.83	90.02
14	1	1	−1	−1	7.11	11.72	12.45	15.05
15	0	0	−2	0	25.08	46.50	47.66	47.26
16	0	0	0	0	47.91	47.81	68.44	68.40
17	−1	−1	−1	−1	73.53	73.41	81.16	80.79
18	1	−1	1	1	18.81	21.63	24.16	32.91
19	0	−2	0	0	53.59	50.98	73.33	64.17
20	0	0	2	0	55.89	56.50	71.88	61.55
21	−1	1	−1	1	69.41	69.25	76.29	76.18
22	−1	1	1	−1	65.42	64.09	77.04	76.25
23	−1	1	−1	−1	57.94	58.32	72.12	68.40
24	−1	1	1	1	76.66	74.73	81.62	83.40
25	1	1	1	1	14.06	17.47	20.66	26.63
26	0	0	0	0	47.51	47.81	68.36	68.40
27	1	−1	−1	−1	10.30	15.43	17.91	21.22
28	−1	−1	1	−1	83.31	80.41	85.16	87.16
29	0	0	0	0	47.91	47.81	68.44	68.40
30	1	−1	−1	1	12.83	17.41	20	26.4
31	0	0	0	0	47.91	47.81	68.44	68.40

plan showing the coded value of the variables together with dye removal performance for RB5 and RR198 are given in Table II.

RESULTS AND DISCUSSION

Chemical Characterization of Chitosan-PPI Dendrimer Hybrid

The FTIR was prepared to determine the presence of functional groups in chemical structure of the pure chitosan, Ch-g-Ea, and CS-PPI (Figure 3). The FTIR spectrum of pure chitosan [Figure 3(a)] revealed differences from that of Ch-g-Ea [Figure 3(b)]. The main differences were: decreasing the peak intensity from 1.21 (chitosan) to 0.3 (Ch-g-Ea); converting the wide and double shoulder of peak at 3449 cm^{-1} corresponding to the stretching vibration of hydroxyl, amino and amide groups to single shoulder at wave number (3409 cm^{-1}) which indicated the strong interaction between amine groups and Ea (Michael reaction); increasing the peak intensity related to aliphatic component at 2916 cm^{-1}; and observing carbonyl group of the carboxylic acid at 1700 cm^{-1}.[12,47] While, the FTIR spectrum of chitosan itself showed some features of amide groups: amide I and amide II bands at 1450–1650 cm^{-1}.[29,30] The decrease of the band related to primary NH_2 groups at 1450–1650 cm^{-1}; 3300–3500 cm^{-1}. The peak located at 1074 cm^{-1} assigned to C—O stretching and after modification remained unchanged.[31] In addition, by comparison of the spectrum of Ch-g-Ea (curve b) and CS-PPI (curve c) in Figure 3, one can deduce that bound between PPI dendrimer and Ch-g-Ea is formed chemically. This is supported by presence of the amine double shoulder of peak at 3449 cm^{-1} and amide I and amide II bands at 1450–1650 cm^{-1}.

^{1}H-NMR and ^{13}C-NMR spectra for components (Ch-g-Ea and CS-PPI) were obtained on a Bruker AQS AVANCE 500 MHz spectrometer.

Selected data for Ch-g-Ea: ^{1}HNMR: δ_H (DCl/D_2O) 1.27 (s, 3.51 H, CH_3 of CO_2Et), 2.06 and 2.09 (s, 0.31 H, NHAc and AcOH), 2.91 (s, 2.6 H, —CH_2—CO_2R), 3.31 (br, 0.85 H, H-2 of N-alkylated GlcN), 3.6–4.1 (m, *N*—CH_2— of *N*-alkyl group, H-2 of GlcNAc, H-3,4,5,6 of GlcN and Glc- NAc), 4.24 (d, 2.34 H, —CH_2— of CO_2Et), 4.60 (br, 0.15 H, H-1 of GlcNAc), 4.90–5.15 (m, H-1 of *N*-alkylated and *N*,*N*-dialkylated GlcN).

^{13}C-NMR (D_2O): δ_C (0.1 M DCl/D_2O) 25.1 (NHAc), 32.7 (NH—CH_2—), 45.8 (—CH_2—COOEt), 51.9 (COOEt), 58.8 (C-2 of GlcN and GlcNAc), 63.0 and 63.6 (C-6), 64.8 (C-2 of *N*-alkylated GlcN), 72.0–73.5 (C-3), 77.7 (C-5), 79.5 (C-4), 99.3 (C-1 of *N*-alkylated GlcN), 100.4 (C-1 of GlcN), 104.2 (C-1 of GlcNAc), 176.0 (NHCO), 177.3 (COOEt).

Selected data for CS-PPI: ^{1}H-NMR (0.5 M DCl/D_2O) δ_H 1.96 (s, 1.9 H, CH_2CH_2N), 2.10 (s, 0.6 H, NHAc), 2.90 (t, 4.2 H, CH_2CO), 3.12 (t, 4.2 H, $CONHCH_2$), 3.35 (br, H-2 of GlcN-R and CH_2CH_2N), 3.63 (m, CH_2 and CH_2NH_2), 3.7–4.0 (brm, H-2 of GlcNAc, H-3,4,5,6 of chitosan), 4.50 (br, H-1 of GlcNAc), 5.01 (br, H-1 of $GlcNR_2$), 5.21 (br, H-1 of GlcN-R).

^{13}C-NMR (0.5 M DCl/D_2O) δ_C 21.7 (CH_2CH_2N), 24.5 (NHAc), 30.3 (CH_2CO), 37.1 (CH_2-NH_2), 43.6 ($CONHCH_2$), 50.8 (NCH_2), 53.8 (CH_2N), 61.9 (C-6 of sugar backbone), 62.8 (C-2), 75.1 (C-3), 78.3 (C-5), 80.9 (C-4), 100.6 (C-1), 173.4 (CONH), 179.0 (NHAc).

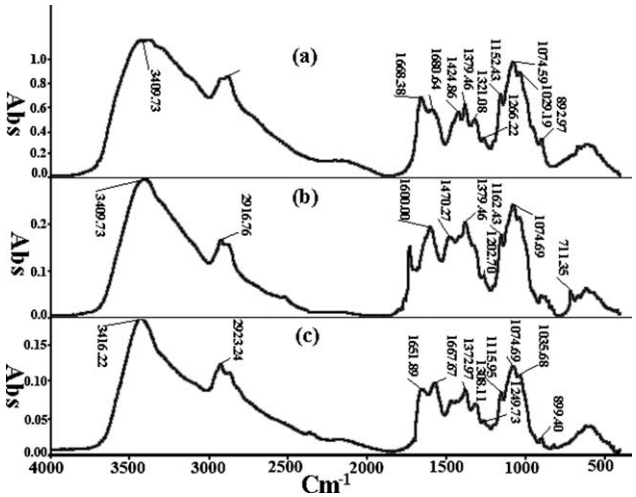

Figure 3. FTIR spectra of (a) chitosan, (b) Ch-g-Ea, and (c) CS-PPI.

Development of the Regression Model Equation

The statistical combinations of the major parameters together with the maximum observed and predicted to dye removal efficiencies are listed in Table II for both dyes. The regression coefficients of the response function, the *t* and *P*-values for RB5 and RR198 dye removal performances using CS-PPI are indicated in Table III. According to the RSM results, the regression model equation regardless the significance of the coefficients for both dyes are developed and represented in the following Equations:

Regression equations for RB5 and RR198

$$\eta_{RBS} = (47.8100) + (-28.8079X_1) + (-4.81208X_2) + (2.49958X_3) + (3.15292X_4) \quad (2)$$

$$\eta_{RR198} = (68.4071) + (-29.0854X_1) + (-4.65042X_2) + (3.57208X_3) + (3.08208X_4) + (-5.72085X_1^2) + (3.38335X_2^2) + (-3.49835X_3^2) \quad (3)$$

Validation of the Model

Analysis of Variance. The analysis of variance (ANOVA) data for both dyes are indicated in Table IV. The models' *P*-value of 0.000 ($P < 0.05$) for both dyes implies that the second-order polynomial models [eqs. (2) and (3)] were highly remarkable and well fitted to the experimental results. The accuracy of the models was further checked by the coefficient of determination R^2-values. According to the ANOVA results, the models present high R^2-value of 98.39% and 96.33% for RB5 and RR198 dyes removal using CS-PPI, respectively. These results signify that the accuracy of the polynomial models is acceptable. In addition, a reasonable conformity with the adjusted determination coefficient is required. In this study, the adjusted R^2-values (96.98% for RB5 and 93.13% for RR198) were high and close to the R^2-

Table III. Estimated Regression Coefficients and Corresponding *t* and *P*-values for two dyes

	Coefficient		Standard deviation		*t*		*P*	
Term	RB5	RR198	RB5	RR198	RB5	RR198	RB5	RR198
Constant	47.81	68.4071	2.075	2.659	23.04	25.726	0.000	0.000
X_1	−28.80	−29.0854	1.121	1.436	−25.71	−20.254	0.000	0.000
X_2	−4.81	−4.6504	1.121	1.436	−4.29	−3.238	0.001	0.005
X_3	2.49	3.5721	1.121	1.436	4.680	2.487	0.040	0.024
X_4	3.15	3.0821	1.121	1.436	2.814	2.146	0.012	0.048
X_1X_1	−39.01	−5.7291	1.027	1.316	−0.380	−4.355	0.709	0.000
X_2X_2	−1.61	−3.3916	1.027	1.316	−1.570	−2.578	0.136	0.020
X_3X_3	0.92	−3.5066	1.027	1.316	0.90	−2.665	0.382	0.017
X_4X_4	−1.2814	−2.6316	1.027	1.316	−1.248	−2.000	0.230	0.063
X_1X_2	2.8431	1.5381	1.372	1.759	2.072	0.875	0.055	0.395
X_1X_3	−0.6194	0.1744	1.372	1.759	−0.451	0.099	0.658	0.922
X_1X_4	−2.0444	−1.0131	1.372	1.759	−1.490	−0.576	0.156	0.573
X_2X_3	−0.3069	0.3519	1.372	1.759	−0.224	0.200	0.826	0.844
X_2X_4	0.1956	−0.3781	1.372	1.759	0.143	−0.215	0.888	0.832
X_3X_4	−0.0744	−0.1394	1.372	1.759	−0.054	−0.079	0.957	0.938

value that ensured a satisfactory adjustment of the polynomial model to the experimental data.

Residual Plots. The plots of residuals against fitted values and the normal probability plots for RB5 and RR198 are presented in Figure 4. The normality assumption for both dyes was relatively satisfied as the points in the plots formed fairly straight. The acceptability of the models fit was also checked by the plots of residuals versus fits. For a model to be reliable, none of these series of increasing or decreasing points, patterns such as increasing residuals with increasing fits and a predominance of positive or negative residuals should be found. Both plots trends observed in Figure 4 reveal reasonably well-behaved residuals for RB5 and RR198. So, it can be concluded that the practical model is adequate to illustrate the removal by RSM for both studied dyes in this research.

Response Surface Plotting for Estimation of Operating Variables

Effect of Initial pH. pH is a major factor which affects to dye adsorption and can influence properties of the adsorbent as well as adsorbate speciation. Figure 5 represents the response surface plots of the initial pH (X_1) and time contact (X_3) on dye removal performance using CS-PPI, respectively. As shown, the decrease of initial pH was useful to enhance the dye removal performance in both dyes in which several reasons may be mentioned to this trend. In general, according to literature, at lower pH more protons will be available to protonate the amino groups of chitosan and PPI to form NH_3^+ groups, thereby increasing electrostatic attractions between negatively charged dye anions ($R–SO_3^-$]) and positively charged adsorption sites and causing an increase in dye adsorption. This explanation agrees with our data concerning the pH effect. The high

Table IV. ANOVA of Removal Performance for RB5 and RR198: Effect of pH, Initial of Dye Concentration, Time, and Temperature

	Degree of Freedom (DF)		Sum of Squares (SS)		Mean Square (MS)		$F_{Statistics}$		*P*	
Source	RB5	RR198	RB5	RR198	RB5	RR198	RB5	RR198	RB5	RR198
Model	14	14	21,219.8	22,848.9	1515.70	1631.63	50.30	32.97	0.000	0.000
Linear	4	4	20,861.8	21,356.3	5215.45	5339.08	173.08	107.87	0.000	0.000
Square	4	4	153.4	1427.2	38.36	356.80	7.21	7.24	0.321	0.002
Interaction	6	6	204.6	59.3	34.1	9.89	1.13	0.20	0.388	0.972
Residual error	25	16	482.1	791.9	30.13	49.49				
Lack of fit	10	10	482.0	791.9	48.20	79.19	2065.6	22261.9	0.000	0.000
Pure error	6	6	0.1	0.0	0.02	0.00				
Total	30	30	21,701.9	23,634.8						

RB5: $S = 5.48938$; PRESS = 2776.47.
R-Sq = 97.78%; *R*-Sq (pred.) = 87.21%; *R*-Sq (adj.) = 95.83%.
RR198: S = 7.03523; PRESS = 4561.32.
R-Sq = 96.65%; R-Sq (pred.) = 80.70%; *R*-Sq (adj.) = 93.72%.

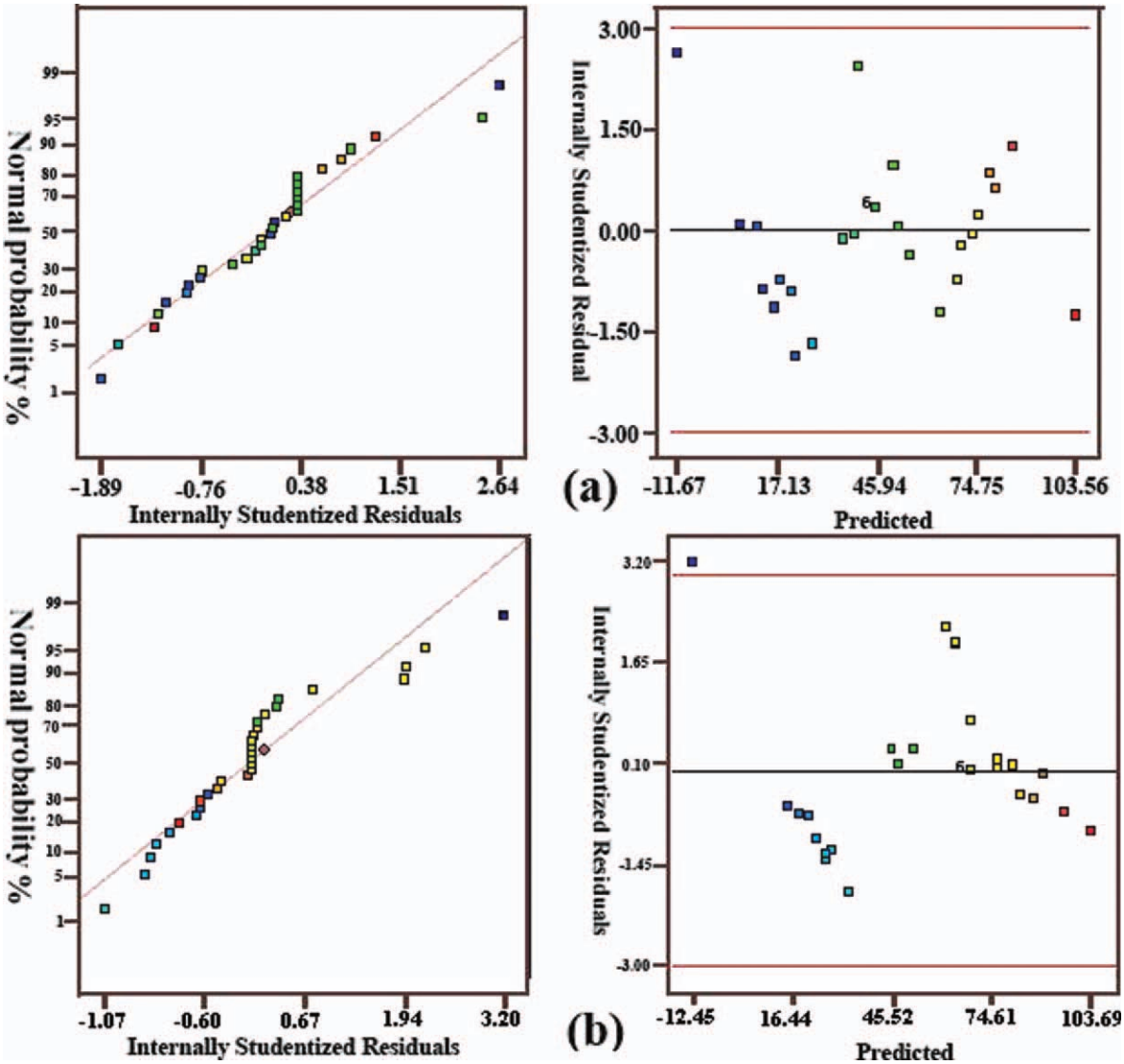

Figure 4. Normal probability plot and residual versus fits for (a) RB5 and (b) RR198. [Color figure can be viewed in the online issue, which is available at wileyonlinelibrary.com.]

adsorption capacity is due to the strong electrostatic interaction between the $-NH_3^+$ of CS-PPI hybrid and dye anions.[18,48] Also, CS-PPI contains of various functional groups such as amino, hydroxyl and carbonyl which could be affected by the pH of solutions. The maximum dye adsorption occurred at pH 2. In this pH, a significantly high electrostatic attraction exists between the positively charged surfaces of the adsorbent, due to the ionization of functional groups of adsorbent and negatively charged anionic dye. As the pH of the system increases, the numbers of negatively charged sites are increased. A negatively charged site on the adsorbent does not favored the adsorption of anionic dyes due to the electrostatic repulsion. The effective pH was 2 and it was used in further studies.

The comparison of dye removal ability by the three studied adsorbents (CS-PPI, chitosan, and dendrimer) show that chitosan and dendrimer are capable to eliminate quantities of dyes from the solutions with high quantity at pH = 2, while CS-PPI can be used to high remove dyes from effluent in various pH at acidic ranges (Table V) which can be related to the increased number of suitable conformation of additional cavities in this adsorbent. The obtained results confirm that the modification of chitosan by dendrimer (PPI, $G = 2$) can reduce the limitation of chitosan and dendrimer in using this environmentally friendly natural components for impurity removal from the polluted effluents.

Effect of Dye Concentration. Figure 6 presents the 3D plots showing the effects of concentration of dye (X_2) and time contact (X_3) on the decolorization of RB5 and RR198 dye solutions using CS-PPI, respectively. As shown in Figure 6, with the increase of concentration of dye, the removal performance steadily decreased for both dyes but when time contact raised, the removal performance steadily decreased for both dyes was high. The amount of the dye adsorbed onto biopolymer increased with an increase in the initial dye concentration of

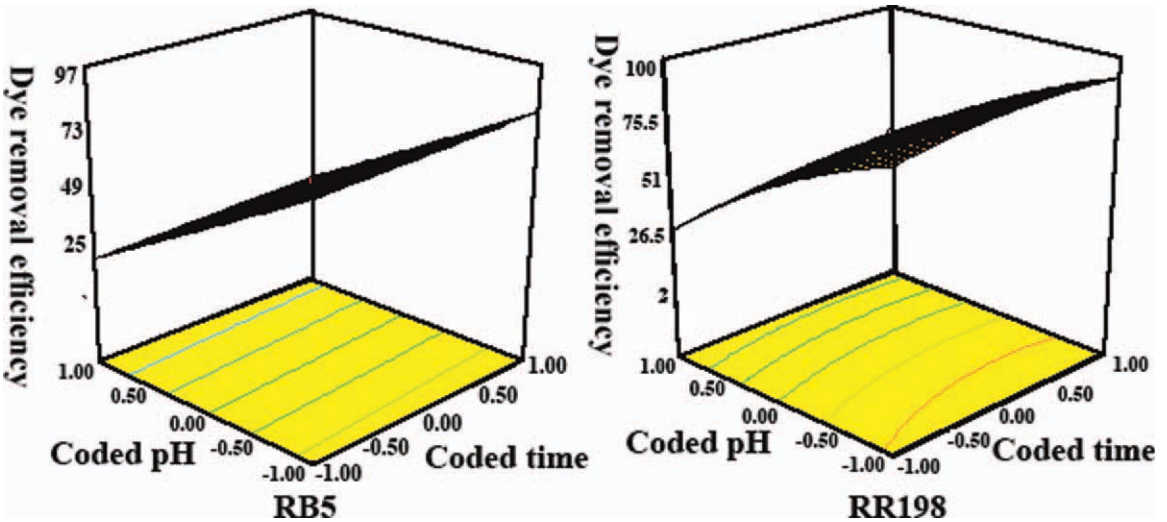

Figure 5. Effects of the initial pH and time on the removal dyes performance. [Color figure can be viewed in the online issue, which is available at wileyonlinelibrary.com.]

solution if the amount of adsorbent was kept unchanged. This is attributable to the increase in the driving force of the concentration gradient with the higher initial dye concentration. At a low initial concentration, the adsorption of dyes by biopolymer is very intense and reaches equilibrium very quickly. [21] At higher concentrations, the number of available adsorption sites becomes lower and subsequently the removal of dyes depends on the initial concentration.

Effect of Temperature. The studies relating the effect of temperature on adsorption was carried out at five different temperatures (30–50°C). The results on dye adsorption at these temperatures would increase the mobility of the large dye ion and also produces a swelling effect within the internal structure of the chitosan, thus enabling the large dye molecule to penetrate further.[49,50] The temperature affects the adsorption rate by altering the molecular interactions and the solubility.[18] The higher removal owing to rising temperature can be attributed to chemical reaction taking place among the functional groups of the adsorbate/adsorbent and the dye (Figure 7).[18,51]

Effect of Time Contact. Referring to Figures 5–7, the percentage of dye removal increased with increasing time contact for both dyes. In other words, contact time is used to assess the practical application of the adsorption process. It is observed from the graphs that dye adsorption on CS-PPI is a slow process, where the adsorption takes place after 10 min and equilibrium is attained within 30 min. Beyond the equilibrium time, adsorption is found to be nearly constant. It can be attributed that at the initial stage of adsorption vacant surface sites are available, and once equilibrium is attained, the remaining vacant sites are difficult to be occupied, probably caused by the repulsive forces between the molecules on the adsorbent.[51,52]

Process Optimization

To obtain optimal regions for RB5 and RR198 dye removal using CS-PPI, response optimizer searched for a combination of factor levels that satisfy dye removal performance of 96.98% and 99.38% for RB5 and RR198, respectively. These results are consistence with the findings of surface plots analysis. According to the Table VI, CS-PPI for RR198 is more effective than RB5. Finally, these optimal values were further validated by actually carrying out the experiments at the optimal conditions. To increase the accuracy of the data, every experiment was repeated five times and the experimental results given in Table VI are the average values. The experimental checking in these optimal conditions (dye removal performance of 96.98% for RB5 and 99.38% for RR198) confirms good agreements with RSM results.

Table V. Dye Removal Efficiency of Two Reactive Dyes by Adsorbents Under Various pH Values

Adsorbent	Dye	pH	Dye removal efficiency (%)
Chitosan	RB5	2	96.98
		4	20.55
		6	10.59
	RR198	2	97.60
		4	28.93
		6	13.21
Dendrimer	RB5	2	97.38
		4	15.12
		6	1.78
	RR198	2	99.51
		4	21.30
		6	2.01
Chitosan-dendrimer	RB5	2	98.67
		4	77.42
		6	55.89
	RR198	2	99.77
		4	82.21
		6	71.88

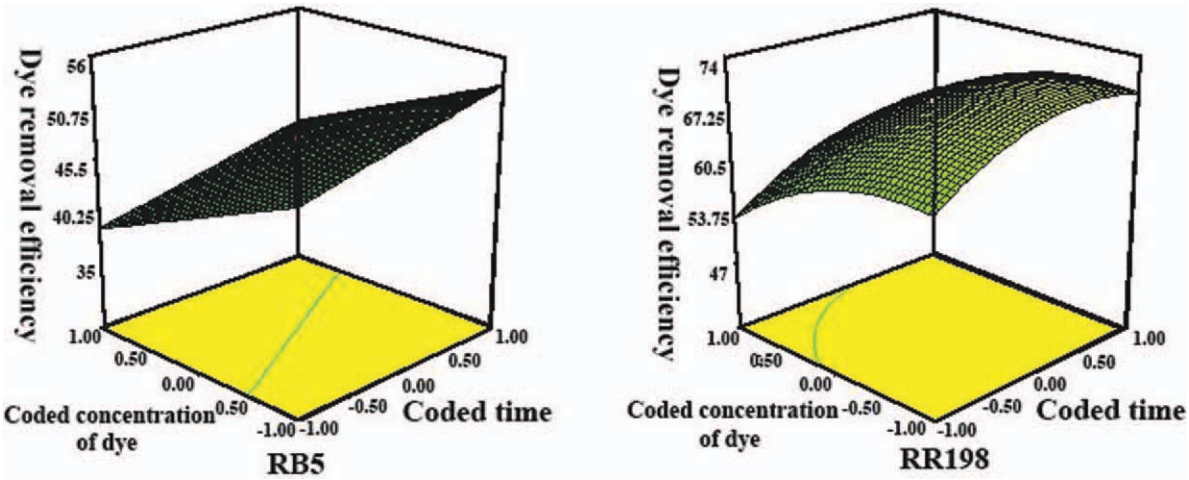

Figure 6. Effects of the concentration of dye and time contact on the removal dyes performance. [Color figure can be viewed in the online issue, which is available at wileyonlinelibrary.com.]

Adsorption Kinetics

Several models can be used to express the mechanism of solute sorption onto an adsorbent. To investigate the mechanism of sorption, characteristic constants of sorption were determined using pseudo-first order equation of Lagergren,[53] pseudo-second order equation[54–56] and intraparticle diffusion model.[55–59]

A linear form of pseudo-first order model [Eq. (4)] is:

$$\log(q_e - q_t) = \log(q_e) - \left(\frac{k_1}{2.303}\right)t \tag{4}$$

where q_e, q_t, and k_1 are the amount of dye adsorbed at equilibrium (mg/g), the amount of dye adsorbed at time t (mg/g) and the equilibrium rate constant of pseudo-first order kinetics (1/min), respectively. The linear fit between the log $(q_e - q_t)$ and contact time (t) under pH_0 2 can be approximated as pseudo-first order kinetics.

Linear form of the pseudo-second order model [Eq. (5)], Ho and MacKay's pseudo-second order model, was illustrated as:

$$\frac{t}{q_t} = \frac{1}{k_2 q_e^2} + \left(\frac{1}{q_e}\right)t \tag{5}$$

where q_e is the amount of dye adsorbed at equilibrium (mg/g) and k_2 is the equilibrium rate constant of the pseudo-second order (g/mg.min). The linear fit between the t/q_t and contact time (t) can be approximated as a pseudo-second order kinetics.

The possibility of intraparticle diffusion resistance affecting adsorption was explored by using the intraparticle diffusion model as indicated by [Eq. (6)]:

$$q_t = k_p t^{0.5} + I \tag{6}$$

where k_p is the intraparticle diffusion rate constant, and I is intercept.

Values of I give an idea about the thickness of the boundary layer, i.e., the larger intercept the greater is the boundary layer

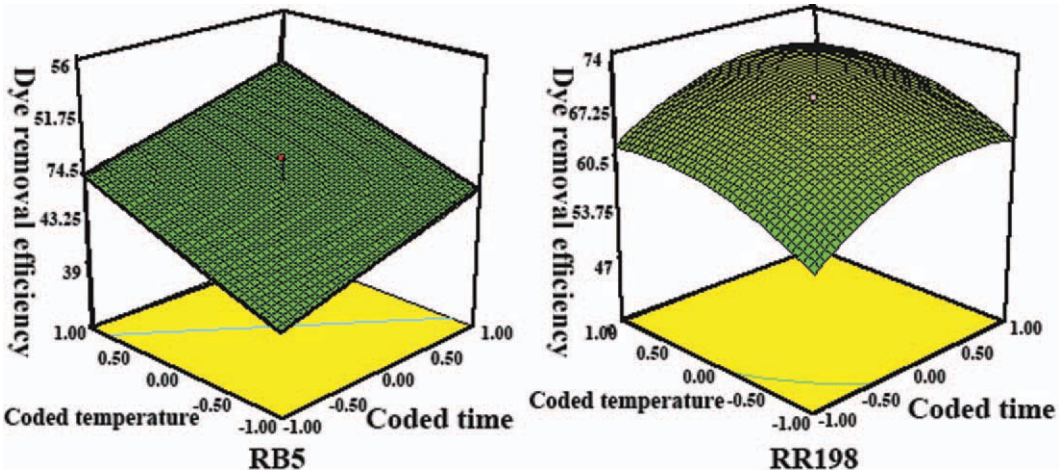

Figure 7. The effects of temperature and time on dyes removal performance. [Color figure can be viewed in the online issue, which is available at wileyonlinelibrary.com.]

Table VI. Optimum Values of the Process Parameter for Maximum Performance

Parameter	Optimum value	
	RB5	RR198
η (efficiency, %)	96.98	99.38
X_1 (pH)	2	2
X_2 (time, min)	30	30
X_3 (C_{dye}, mg/L)	75	75
X_4 (temperature, °C)	40	40

effect. According to this model, the plot of uptake should be linear if intraparticle diffusion is involved in the adsorption process and if these lines pass through the origin then intraparticle diffusion is the rate controlling step.[55–57] When the plots do not pass through the origin, this is indicative of some degree of boundary-layer control and this further show that the intraparticle diffusion is not the only rate limiting step, but also other kinetic models may control the rate of adsorption, all of which may be operating simultaneously.

The values of k_1, k_2, R_1^2, R_2^2, k_p, c, and R_3^2 were calculated and shown in Table VII. Adsorption kinetics of dyes was studied and the rates of sorption were found to be conforming to the pseudo-second order kinetics with good correlation.

Adsorption Isotherms

The adsorption isotherm expresses the relation between the mass of the dye adsorbed at a particular temperature, the pH, particle size, and liquid phase of the dye concentration. Several isotherms such as Langmuir, Freundlich, and Temkin isotherms were investigated. The Langmuir isotherm which has been successfully applied to many sorption processes can be used to explain the sorption of dye on chitosan. A basic assumption of the Langmuir theory is that sorption takes place at specific sites within the adsorbent.[55–57] The Langmuir equation can be written as follows [Eq. (7)][18,53,57]:

$$q_e = \frac{Q_0 K_L C_e}{1 + K_L C_e} \tag{7}$$

where, q_e, C_e, K_L, and Q_0 are the amount of dye adsorbed on CS-PPI at equilibrium (mg/g), the equilibrium concentration of dye solution (mg/L), Langmuir constant (L/g) and the maximum adsorption capacity (mg/g), respectively. The linear form of Langmuir equation is indicated by [Eq. (8)]:

$$\frac{C_e}{q_e} = \frac{1}{K_L Q_0} + \frac{C_e}{Q_0} \tag{8}$$

Also, isotherm data were tested with Freundlich isotherm that can be expressed by [Eq. (9)][18,53,57]:

Table VII. Kinetic Constant for the Pseudo-First and the Pseudo-Second Order and the Intraparticle Diffusion Model in Optimum Values of the Process Parameter

Dye	$C_{solution}$ (mg/L)	$(q_e)_{Exp.}$	Pseudo-first order			Pseudo-second order			Intraparticle diffusion		
			$(q_e)_{Cal.}$	k_1	R_1^2	$(q_e)_{Cal.}$	k_2	R_2^2	k_P	I	R_3^2
RB5	25	1243.35	1059.00	0.093	0.99	1428.57	2×10^{-4}	0.999	145.13	150.3	0.908
	50	2480.05	1678.80	0.070	0.912	2500	8.8×10^{-5}	0.998	280.93	336.66	0.887
	75	3700.13	14,541.19	0.285	0.641	3333.33	4.5×10^{-4}	0.999	408.04	816.6	0.747
	100	4843.75	6205.83	0.139	0.823	5000	6.6×10^{-5}	0.999	548.82	787.68	0.848
	125	5841.09	5776.96	0.092	0.998	10,000	8.3×10^{-6}	0.998	693.51	500.94	0.945
RR198	25	1245.83	895.36	0.091	0.958	1250	2.4×10^{-4}	0.999	140.92	200	0.853
	50	2493.75	1561.70	0.094	0.928	2500	1.6×10^{-4}	0.999	278.29	457.45	0.814
	75	3735.41	2258.91	0.168	0.957	3333.33	4.5×10^{-4}	0.999	415.76	808.4	0.757
	100	4814.58	3812.41	0.080	0.974	5000	6×10^{-5}	0.999	555.86	574.66	0.91
	125	5666.66	6359.16	0.109	0.994	10,000	8.3×10^{-6}	0.996	678.63	494.05	0.941

Table VIII. Linearized Isotherm Coefficient for Used Two Dyes and Three Adsorbents in Optimum Values of the Process Parameter

Adsorbent	Dye	Langmuir isotherm			Freundlich isotherm			Temkin isotherm		
		q_0	K_L	R_1^2	K_F	n	R_2^2	K_T	B_1	R_3^2
CS-PPI	RB5	6250	0.145	0.998	3105.98	2.739	0.937	23.799	1121.8	0.997
	RR198	5882.35	0.340	0.997	3483.37	4.132	0.756	156.56	772.42	0.902
Chitosan	RB5	5555.55	0.720	0.999	2123.24	2.77	0.894	10.234	1031.2	0.952
	RR198	5263.15	0.422	0.997	1599.55	2.570	0.845	4.516	1071.2	0.926
Dendrimer PPI ($G = 2$)	RB5	5882.35	0.809	0.997	2338.83	2.695	0.927	11.854	1087.72	0.972
	RR198	5555.55	0.514	0.999	1857.80	2.597	0.923	6.435	1087.3	0.974

Table IX. Adsorption Capacities for the Removal of Reactive Dyes by Other Adsorbents

Adsorbate	Adsorbent	q_0	Reference
Reactive red 120	*Hydrilla verticillata*	120.85 mg/g	60
Reactive red 198	*Potamogeton crispus*	44.2 mg/g	61
Reactive red 120	*Spirogyra majuscula*	351.97mg/g	62
Reactive red 239	Modified sepiolite	108.8 mg/g	63
Remazol red RB	Yeast (*Saccharomyces cerevisiae*)	48.8 mg/g	64
Reactive red 120	Metal hydroxide sludge–	48.31 mg/g	65
Reactive red 189	Crosslinked chitosan bead	1936 mg/g	23
Reactive blue 2,	Chitosan bead (chemically crosslinked)	2498 mg/g	66
Reactive red 222	Chitosan bead (lobster)	1037 mg/g	67

$$q_e = K_F C_e^{1/n} \quad (9)$$

where, K_F is the adsorption capacity at unit concentration and $1/n$ is adsorption intensity. $1/n$ values indicate the type of isotherm to be irreversible ($1/n = 0$), favorable ($0 < 1/n < 1$) and unfavorable ($1/n > 1$). Equation (10) can be rearranged to a linear form:

$$\log q_e = \log K_F + \frac{1}{n} \log Ce \quad (10)$$

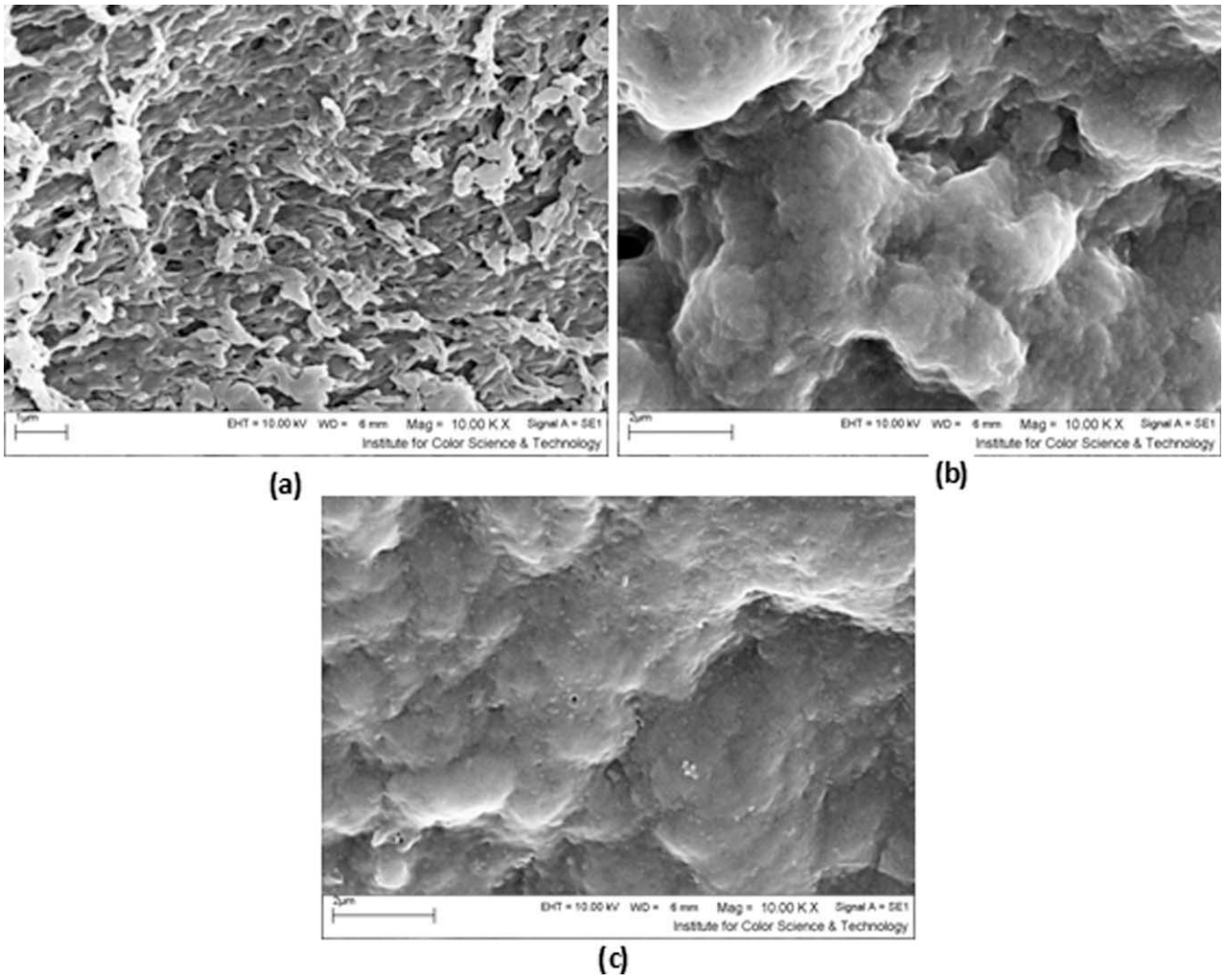

Figure 8. SEM images for CS-PPI: (a) raw CS-PPI; (b) after 30 min adsorption process (RB5) and (c) after 30 min adsorption process (RR198). Conditions: 0.02 g/L.

The Temkin isotherm is given by [Eq. (11)]:

$$q_e = \frac{RT}{b \ln(K_T C_e)} \quad (11)$$

which can be linearized as indicated by [Eq. (12)];

$$q_e = B_1 \ln K_T + B_1 \ln C_e \quad (12)$$

where [Eq. (13)];

$$B_1 = \frac{RT}{b} \quad (13)$$

The Temkin isotherm equation assumes that the heat of adsorption of all the molecules in layer decreases linearly with coverage due to adsorbent–adsorbate interactions, and that the adsorption is characterized by an uniform distribution of the bonding energies, up to some maximum binding energy.[58,59] A plot of q_e versus ln C_e enables the determination of the isotherm constants B_1 and K_T from the slope and the intercept, respectively. K_T is the equilibrium binding constant (L/mol) corresponding to the maximum binding energy, and constant B_1 is related to the heat of adsorption. Also, T, R, and b are the absolute temperature (K), the universal gas constant (8.314 J/mol K) and a constant related to heat adsorption, respectively.

The q_0, K_L, R_1^2, K_F, n, R_2^2, K_T, B_1 and, R_3^2 correlation coefficients for Langmuir, Freundlich and Temkin isotherms are given in Table VIII. The data of Table VIII indicate that the Langmuir isotherm is the most appropriate to describe the adsorption of RB5 and RR198 on CS-PPI. Comparison of q_0 values for the three adsorbent indicate that the CS-PPI has more capacity for elimination of reactive dyes in colored solution. In general, Comparison of q_0 values of the three adsorbents showed that they follow the order of CS-PPI > dendrimer > chitosan.

Adsorption capacities for the removal of reactive dyes by other adsorbents have been shown in Table IX. Data in Table IX shows the equilibrium capacity of CS-PPI is considerable higher than other adsorbents.

SEM Analysis

SEM has been a main instrument for characterizing the surface morphology and essential physical properties of the material surface. It is valuable for determining the particle shape, porosity, and appropriate size distribution of the adsorbent. Scanning electron micrographs of raw CS-PPI and adsorbed CS-PPI with RB5 and RR198 are given in Figure 8. It is clear from Figure 8, CS-PPI has considerable numbers of pores where, there is a good possibility for reactive dyes to be trapped and adsorbed in its pores. The SEM pictures of CS-PPI samples show very distinguished dark spots which can be taken as a criterion for successful adsorption of reactive dye molecules in the cavities and pores of this prepared adsorbent.

CONCLUSIONS

In this research, the synthesis, characterization, and dye adsorption properties of biocompatible biopolymer CS-PPI was investigated. CS-PPI was characterized by using FTIR, ^{1}H-NMR, ^{13}C-NMR, and SEM. This study indicated that the RSM was one of the suitable methods to optimize the best operating conditions to maximize the dye removal. Graphical response surface was used to locate the optimum point. Results showed that the decrease of initial pH was beneficial for enhancing dye removal performance in both dyes. An optimum condition for the decolorization process using RSM was achieved at initial pH value of 2, concentration of dye of 75 g/L, time contact of 30 min and temperature of 40°C for both dyes. Adsorption isotherm study indicated that RB5 and RR198 absorption were reasonably correlated by Langmuir model. The experimental data fitted well to pseudo-second order kinetic model. The findings of this study revealed that CS-PPI can be as a suitable environmentally friendly adsorbent with high removal potential for reactive dyes from colored textile effluents.

REFERENCES

1. Elwakeel, K. Z. *J. Hazard. Mater.* **2009,** *167*, 383.
2. Piccin, J. S.; Vieira, M. L. G.; Gonc alves, J.; Dotto, G. L.; Pinto, L. A. *J. Food. Eng.* **2009,** *95*, 16.
3. Mahmoodi, N. M.; Arami, M. *Chem. Eng. J.* **2009,** *146*, 189.
4. Mahmoodi, N. M.; Arami, M. *J. Photochem. Photobiol. B* **2009,** *94*, 20.
5. Mahmoodi, N. M.; Arami, M. *J. Appl. Polym. Sci.* **2008,** *109*, 4043.
6. Mahmoodi, N. M.; Arami, M. *J. Photochem. Photobiol. A* **2006,** *182*, 60.
7. Mahmoodi, N. M.; Arami, M.; Limaee, N. Y.; Tabrizi, N. S. *Chem. Eng. J.* **2005,** *112*, 191.
8. Mahmoodi, N. M.; Arami, M.; Limaee, N. Y.; Tabrizi, N. S. *J. Colloid Interface Sci.* **2006,** *295*, 159.
9. Mahmoodi, N. M.; Arami, M.; Limaee, N. Y.; Gharanjig, K.; Ardejani, F. D. *Colloids Surf. A* **2006,** *290*, 125.
10. Mahmoodi, N. M.; Limaee, N. Y.; Arami, M.; Borhany, S.; Mohammad-Taheri, M. *J. Photochem. Photobiol. A* **2007,** *189*, 1.
11. Maljaei, A.; Arami, M.; Mahmoodi, N. M. *Desalination* **2009,** *249*, 1074.
12. Salehi, R.; Arami, M.; Mahmoodi, N. M.; Bahrami, H.; Khorramfar, S. *Colloids Surf. B* **2010,** *80*, 86.
13. Blackburn, S. R. *Environ. Sci. Technol.* **2004,** *38*, 4905.
14. Gupta, V. K.; Suhas. *J. Environ. Manage.* **2009,** *90*, 2313.
15. Du, G.; Li, Y.; Tao, Y.; Deng, H.; Luo, X.; Yang, J. *Carbohydr. Polym.* **2010,** *82*, 706.
16. Shimei, X.; Jingli, W.; Ronglan, W.; Jide, W. *Carbohydr. Polym.* **2006,** *66*, 55.
17. Srinivasan, A.; Viraraghavan, T. *J. Environ. Manage.* **2010,** *91*, 1915.
18. Annadurai, G. *Iran Polym. J.* **2002,** *11*, 237.
19. Cestari, A. R.; Vieira, E. F. S.; dos Santos, A. G. P.; Mota, J. A.; de Almeida, V. P. *J. Colloid. Int. Sci.* **2004,** *280*, 380.
20. Rinaudo, M. *Prog. Polym. Sci.* **2006,** *31*, 603.
21. Crini, G.; Badot, P. M. *Prog. Polym. Sci.* **2008,** *33*, 399.

22. Gibbs, G.; Tobin, J. M.; Guibal, E. *Ind. Eng. Chem. Res.* **2004,** *43*, 1.
23. Chiou, M. S.; Li, H. Y. *J. Hazard. Mater. B* **2002,** *93*, 233.
24. Alves, N. M.; Mano, J. F. *Int. J. Biol. Macromol.* **2008,** *43*, 401.
25. Zainal, Z.; Hui, L. K.; Hussein, M. Z. O.; Abdullah, A. H.; Hamadneh, I. R. *J. Hazard. Mater.* **2009,** *164*, 138.
26. Chen, J. Y.; Zhou, P. J.; Li, J. L.; Wang, Y. *Carbohydr. Polym.* **2008,** *72*, 128.
27. Zhu, H.; Jiang, R.; Xiao, L.; Chang, Y.; Guan, Y.; Li, X.; Zeng, G. *J. Hazard. Mater.* **2009,** *169*, 933.
28. Sashiwa, H.; Shigemasa, Y.; Roy, R. *Macromolecules* **2000,** *33*, 6913.
29. Sashiwa, H.; Shigemasa, Y.; Roy, R. *Macromolecules* **2001,** *34*, 3905.
30. Sashiwa, H.; Shigemasa, Y.; Roy, R. *Macromolecules* **2001,** *34*, 3211.
31. Sashiwa, H.; Shigemasa, Y.; Roy, R. *Carbohydr. Polym.* **2002,** *49*, 195.
32. Sashiwa, H.; Yajima, H.; Aiba, S. *Biomacromolecules* **2003,** *4*, 1244.
33. Sashiwa, H.; Yajima, H.; Ichinose, Y.; Yamamori, N.; Sunamoto, J.; Aiba, S. *Chitin Chitosan Res.* **2003,** *9*, 45.
34. Tsubokawa, N.; Takayama, T. *React. Funct. Polym.* **2000,** *43*, 341.
35. Astruc, D.; Boisselier, E.; Ornelas, C. *Chem. Rev.* **2010,** *110*, 1857.
36. Hay, G.; Mackay, M. E.; Hawker, C. J. *J. Polym. Sci. Part B: Polym. Phys.* **2001,** *39*, 1766.
37. Klajnet, B.; Bryszewska, M. *Acta Biochem Pol* **2001,** *48*, 199.
38. Froehling, P. E. *Dyes Pigments* **2001,** *48*, 187.
39. Burkinshaw, S. M.; Mignanelli, M.; Froehling, P. E.; Bide, M. *J. Dyes Pigments* **2000,** *47*, 259.
40. Newkome, G. R.; Shreiner, C. D. *Polymer* **2008,** *49*, 1.
41. Tomalia, D. A.; Frechet, J. M. *J. Polym. Sci. Part A: Polym. Chem.* **2002,** *40*, 2719.
42. Mahmoodi, N. M.; Hayati, B.; Arami, M.; Mazaheri, F. *J. Chem. Eng. Data* **2010,** *55*, 4660.
43. Klaykruayat, B.; Siralertmukul, K.; Srikulkit, K. *Carbohydr. Polym.* **2010,** *80*, 197.
44. Ravikumar, K.; Ramalingam, S.; Krishnan, S.; Balu, K. *Dyes Pigments* **2006,** *70*, 18.
45. Silva, J. P.; Sousa, S.; Rodrigues, J.; Antunes, H.; Porter, J. J.; Gonçalves, I.; Ferreira- Dias, S. *Sep. Purif. Technol.* **2004,** *40*, 309.
46. Sashiwa, H.; Kawasaki, N.; Nakayama, A.; Muraki, E.; Yajima, H.; Yamamori, N.; Ichinose, Y.; Sunamoto, J.; Aiba, S. *Carbohydr. Res.* **2003,** *338*, 557.
47. Wu, H.; Zhang, J.; Xiao, B.; Zan, X.; Gao, J.; Wan, Y. *Carbohydr. Polym.* **2011,** *83*, 824.
48. Crini, G.; Gimbert, F.; Robert, C.; Martel, B.; Adam, O.; Crini, N. M.; Giorgi, F. D.; Badot, P. M. *J. Hazard. Mater.* **2008,** *153*, 96.
49. Yoshida, H.; Okamoto, A.; Kataoka, T. Chem. Eng. Sci. **1993,** *48*, 2267.
50. Woodard, F.Industrial Waste Treatment Handbook; Butterworth-Heinemann, Boston, **2001.**
51. Chiou, M. S.; Li, H. Y. *Chemosphere* **2003,** *50*, 1095.
52. Alley, E. R.Water Quality Control Handbook, Vol. *8*; McGraw-Hill Professional, London, **2000.**
53. Langergren, S.; Svenska, B. K. *Veternskapsakad Handl* **1898,** *24*, 1.
54. Ho, Y. S. Ph.D. Thesis, Adsorption of heavy metals from waste streams by peat. The University of Birmingham, Birmingham, UK, **1995.**
55. Ho, Y. S. *Adsorption* **2001,** *7*, 139.
56. Ho, Y. S.; McKay, G. *Process Biochem.* **1999,** *34*, 451.
57. Ozcan, A.; Ozcan, A. S. *J. Hazard. Mater.* **2005,** *125*, 252.
58. Senthilkumaar, S.; Kalaamani, P.; Porkodi, K.; Varadarajan, P. R.; Subburaam, C. V. *Bioresour. Technol.* **2006,** *97*, 1618.
59. Weber, W. J.; Morris, J. C. *J. Sanit. Eng. Div. Am. Soc. Civil Eng.* **1963,** *89*, 31.
60. Naveen, N.; Saravanan, P.; Baskar, G.; Renganathan, S. *J. Taiwan Inst. Chem. Eng.* **2011,** *42*, 463.
61. Gulnaza, O.; Sahmurova, A.; Kama, S. Chem. Eng. J. **2011,** *174*, 579.
62. Celekli, A.; Yavuzatmaca, M.; Bozkurt, H. *Chem. Eng. J.* **2009,** *152*, 139.
63. Ozdemir, O.; Armagan, B.; Turan, M.; Celik, M. S. *Dyes Pigments* **2004,** *62*, 49.
64. Aksu, Z.; Donmez, G. *Chemosphere* **2003,** *50*, 1075.
65. Netpradit, S.; Thiravetyan, P.; Towprayoon, S. *Water Res.* **2003,** *37*, 763.
66. Chiou, M. S.; Ho, P. Y.; Li, H. Y. *Dyes Pigments* **2004,** *60*, 69.
67. Wu, F. C.; Tseng, R. L.; Juang, R. S. *J. Hazard Mater.* **2000,** *73*, 63.